ACSNANO
www.acsnano.org
ARTICLE

Piezopotential-Programmed Multilevel Nonvolatile Memory As Triggered by Mechanical Stimuli

Qijun Sun,[†] Dong Hae Ho,[‡] Yongsuk Choi,[‡] Caofeng Pan,[†] Do Hwan Kim,[∥] Zhong Lin Wang,[†,⊥] and Jeong Ho Cho*[,‡,§]

[†]Beijing Institute of Nanoenergy and Nanosystems, Chinese Academy of Sciences, National Center for Nanoscience and Nanotechnology (NCNST), Beijing 100083, P. R. China

[‡]SKKU Advanced Institute of Nanotechnology (SAINT) and [§]School of Chemical Engineering, Sungkyunkwan University, Suwon, 440−746, Korea

[∥]Department of Organic Materials and Fiber Engineering, Soongsil University, Seoul 156-743, Korea

[⊥]School of Materials Science and Engineering, Georgia Institute of Technology, Atlanta, Georgia 30332−0245, United States

Supporting Information

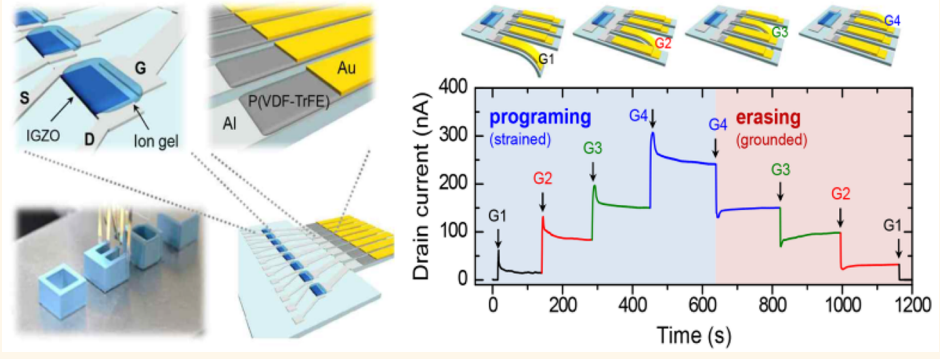

ABSTRACT: **We report the development of a piezopotential-programmed nonvolatile memory array using a combination of ion gel-gated field-effect transistors (FETs) and piezoelectric nanogenerators (NGs). Piezopotentials produced from the NGs under external strains were able to replace the gate voltage inputs associated with the programming/erasing operation of the memory, which reduced the power consumption compared with conventional memory devices. Multilevel data storage in the memory device could be achieved by varying the external bending strain applied to the piezoelectric NGs. The resulting devices exhibited good memory performance, including a large programming/erasing current ratio that exceeded 10^3, multilevel data storage of 2 bits (over 4 levels), performance stability over 100 cycles, and stable data retention over 3000 s. The piezopotential-programmed multilevel nonvolatile memory device described here is important for applications in data-storable electronic skin and advanced human-robot interface operations.**

KEYWORDS: *piezopotential, nonvolatile memory, transistor, nanogenerator, multilevel data storage*

Piezopotentials created in a noncentral symmetry crystal under an external strain offer a low-energy-consumption solution for powering electronic devices.[1−4] Diverse electronic systems that rely on piezopotential power have been prepared and have inspired rapid progress in broad applications ranging from external stimuli sensation to environmental monitoring.[5−9] The feasibility of integrating these devices into in vivo biomedical devices that harvest biochemical energy[10,11] and biomechanical energy[12,13] has been explored. Furthermore, piezopotential inputs created by external stimuli can enable the incorporation of diverse functions into electronic systems to achieve active digital signal/data processing capabilities, such as high-resolution dynamic pressure sensor arrays,[14,15] active and adaptive matrices for tactile imaging,[16] and interactions between machines and humans or the environment.[17] Together, these findings demonstrate the significant promise of piezopotential power for use in multifunctional electronic skin applications.[18−24] However, a key shortcoming of these electronic systems is their

Received: September 1, 2016
Accepted: November 28, 2016
Published: November 28, 2016

DOI: 10.1021/acsnano.6b05895
ACS Nano 2016, 10, 11037−11043

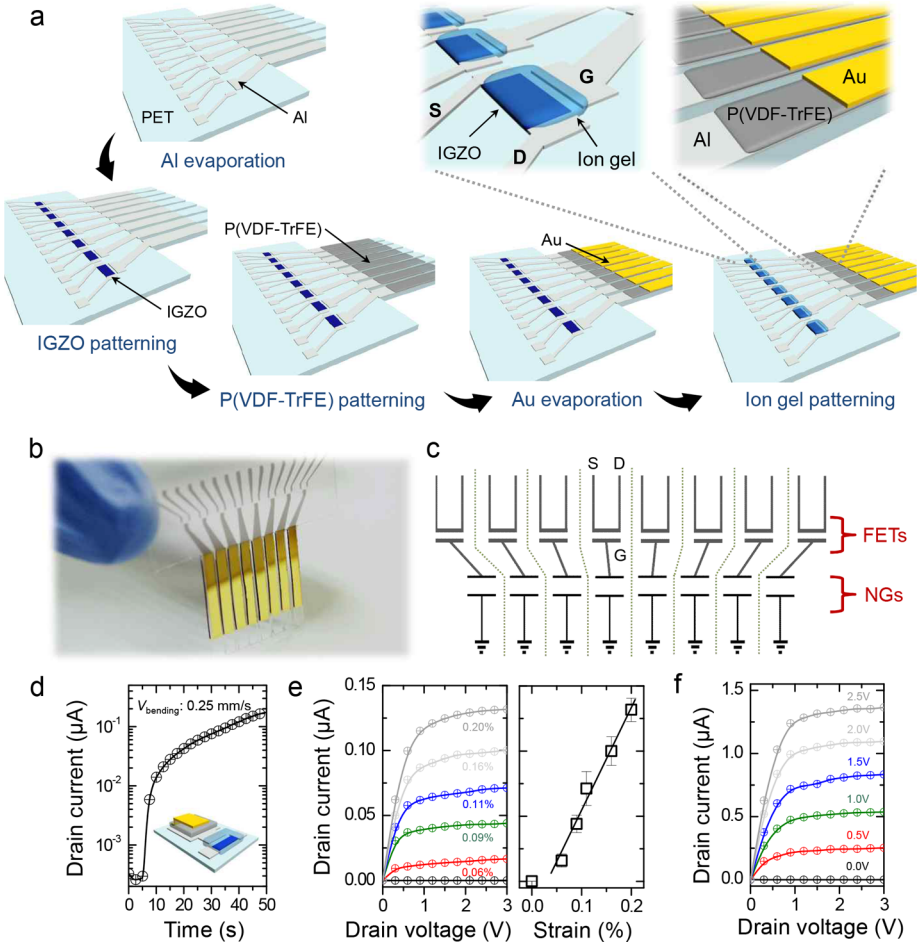

Figure 1. (a) Procedure used to fabricate the piezopotential-programmed multilevel nonvolatile memory array. (b) Photographic image and (c) circuit diagram of the memory array. (d) Drain current−time plot of the piezopotential-powered ion gel-gated IGZO FETs, at a bending speed of 0.25 mm/s. (e) Drain current−drain voltage plot of the piezopotential-powered ion gel-gated IGZO FETs under various strains (left) and drain currents as a function of the applied strain (right). (f) Drain current−drain voltage plot of the ion gel-gated IGZO FETs under various gate voltages.

inability to store sensing signals, which can hinder their use in continuous long-term monitoring and subsequent data processing. Piezoelectric-powered intellective systems should feature both sensing properties and memory functions.[25,26]

Among the different types of memory devices available, transistor-type flash memory is the most widely used form due to its easily integrated structure and nondestructive reading-out characteristics.[27−29] Conventional transistor-type memory operates by conducting data storage/erase processes using charge trapping/releasing at a floating gate inserted between tunneling and blocking gate dielectrics. During this process, a high voltage input is generally applied at the gate electrode to induce charge tunneling through the tunneling dielectrics, which inevitably consumes significant quantities of energy. The preparation of tunneling dielectric and charge trapping layers can complicate device fabrication processes. Previous studies have reported the development of piezoelectrically modulated resistive switching devices, through which the storage/erase access of the memory cell may be programmed under externally applied mechanical modulation.[30] The low programming/erasing current ratio of these devices precluded their use in multilevel data storage applications. Another type of tribotronic transistor memory has been used in mechanical touch monitoring systems, in which the memory is integrated with light-emitting diodes.[31] The complicated programming/erasing operations of this type of device have hindered its use in highly integrated arrays. Therefore, it is critical to develop low power consumption transistor-type memories with simple device geometries through the use of piezoelectric power. Furthermore, the memory device as triggered by mechanical stimuli is of great importance for next frontier in personalized healthcare system by integrating physiological activity detection, data storage, and feedback therapy.

In this article, we demonstrated a piezopotential-programmed nonvolatile memory arrays using a compact combination of ion gel-gated field-effect transistors (FETs) and piezoelectric nanogenerators (NGs). The solution-processed indium−gallium−zinc−oxide (IGZO) and poly(vinylidenefluoride-*co*-trifluoroethylene) [P(VDF-TrFE)] materials were used as the channel layer in the FETs and piezoelectric layer in the NGs, respectively. Piezopotentials produced from the NGs under external strains replaced conventional gate voltage inputs for the programming/erasing operations of the memory, which reduced the power consumption of the devices. The charges in the gate electrode induced by the piezopotentials from the NGs accumulated charge carriers in the transistor channel through the ion gel. By disconnecting the top electrode of the NG from the ground

DOI: 10.1021/acsnano.6b05895
ACS Nano 2016, 10, 11037−11043

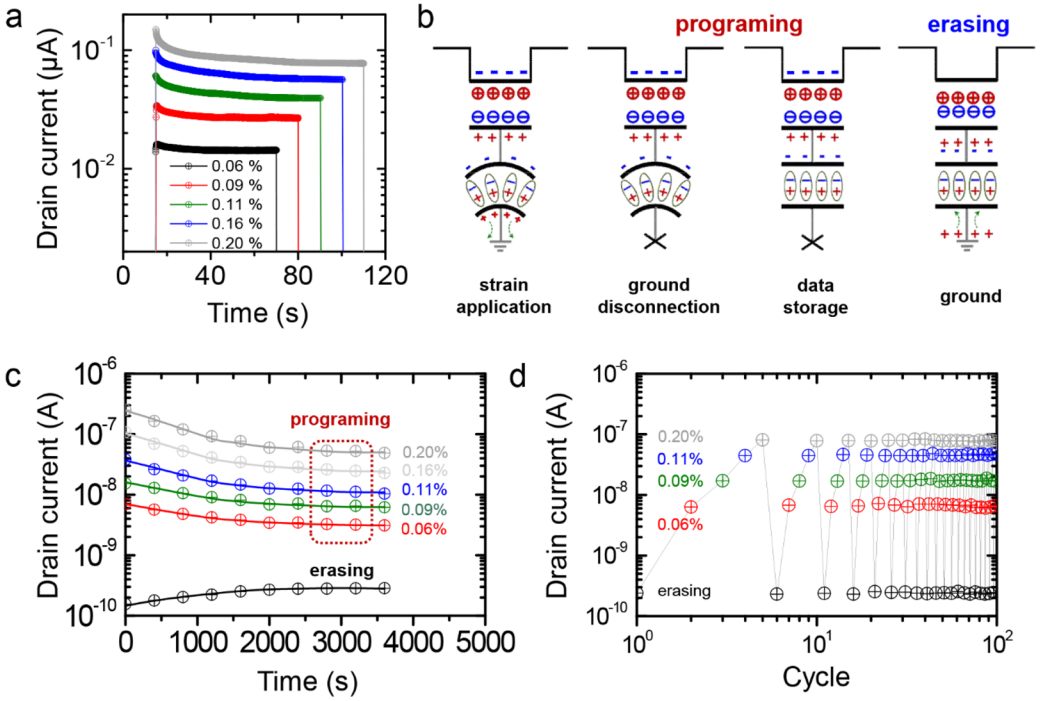

Figure 2. (a) Persistent current characteristics of the piezopotential-programmed nonvolatile memory under various bending strains, from 0.06 to 0.20%. (b) Operation mechanism underlying the piezopotential-programmed nonvolatile memory. (c) Retention time and (d) cyclic endurance tests of the piezopotential-programmed nonvolatile memory.

after bending the device, the as-induced charges could be preserved in the channel, even if the strain were then subsequently released. The resulting persistent current level set "the programmed state" of the device. By contrast, the current level recovered its original value by grounding the top electrode of the NG (reconnecting the top electrode of the NG to the ground), which set the "erased state" of the device. Note that the programming and erasing states of the memory devices were realized through external mechanical stimuli. Multilevel data storage of the memory device was achieved by varying the external bending strains applied to the NGs. The resulting devices exhibited good memory performances, including a large programming/erasing current ratio that exceeded 10^3, multilevel data storage of 2 bits (over 4 levels), performance stability over 100 cycles, and stable data retention over 3000 s. The sensing properties of our memory device were demonstrated using a 2D color map of the alphabet letters "OEDL". The proposed piezopotential-programmed multilevel nonvolatile memory is important for applications in the fields of data-storable electronic skin and advanced human−robot interface operation.

RESULTS AND DISCUSSION

Figure 1a exhibits a schematic diagram of the procedure used to fabricate the piezopotential-programmed nonvolatile memory array. First, a 50 nm thick Al layer was deposited onto a polyethylene terephthalate (PET) substrate to serve as the source-drain and extended coplanar gate electrodes. Indium−gallium−zinc-oxide (IGZO), as the active channel in the FETs, was then spin-coated using the IGZO precursors dissolved in 2-methoxyethanol. The IGZO channel was subsequently irradiated with deep-ultraviolet light, which induced efficient condensation and densification of the IGZO films through photochemical activation at low temperature.[32] The IGZO channels were then patterned by photolithography and chemical etching processes. The piezopotential powering components were integrated onto the extended coplanar Al gate electrodes by depositing a P(VDF-TrFE) layer through a conformable polymeric mask.[33] The deposition of top Au electrodes was subsequently applied. After the electrical poling process, needle-like crystalline domains were observed in the P(VDF-TrFE) film (Figure S1), typical ferroelectric β phases.[34] The output voltages generated from the resulting P(VDF-TrFE) NGs were around 5 V at a strain of 0.2%, as shown in Figure S2. The device was finalized by photopatterning of a high-capacitance ion gel gate dielectric [poly(ethylene glycol) diacrylate] (PEGDA) prepolymer, a 2-hydroxy-2-methylpropiophenone (HOMPP) photoinitiator, and 1-ethyl-3-methylimidazolium bis(trifluoromethanesulfonyl)imide ([EMIM][TFSI]) ionic liquid, in a weight ratio of 7:3:90 across the IGZO channels and a portion of the Al gate electrodes. The insets of Figure 1a display the magnified IGZO FETs (signal reading and storing part) and piezoelectric NGs (powering and sensing parts). The memory array was composed of eight groups of piezopotential-powered FETs, as shown in Figure 1b. Eight IGZO FETs were aligned next to one another and eight NGs were integrated onto their extended gates, respectively. The piezoelectric NGs served to sense the external strains and provide a voltage to gate the FETs, whereas the ion gel-gated IGZO FETs acted as the signal reading and memorizing components. Figure 1c shows an equivalent circuit diagram of the memory device array.

The electrical performance of the single piezopotential-programmed nonvolatile memory was first characterized. The electron mobility of the IGZO FETs calculated from the transfer characteristics in Figure S3 was 4.3 $cm^2/V{\cdot}s$. Figure 1d shows the drain current (I_D) of the piezopotential-gated IGZO FETs as a function of time. The device mounted on a home-built bending machine was bent at a speed of 0.25 mm/s. The

DOI: 10.1021/acsnano.6b05895
ACS Nano 2016, 10, 11037−11043

I_D increased from 2.6×10^{-4} to 0.17 μA as the bending strain increased from 0 to 0.2%. The applied bending strain was calculated from the equations in Figure S4. As the P(VDF-TrFE) NG was subjected to the bending strain, the enhanced piezoelectric potential repelled hole charges to the Al gate electrode. The negative TFSI ions in the ion gel were then attracted to the interface between the Al gate and the ion gel, whereas positive EMIM ions in the ion gel migrated to the interface between the ion gel and the IGZO channel. Electrical double layers (EDLs) formed at both interfaces, as shown in Figure S5a. The formation of EDLs in the ion gel gate dielectrics accumulated electron charges in the IGZO channel (Figure S5b). The left panel of Figure 1e shows an I_D-drain voltage (V_D) plot of the IGZO FETs under different bending strains, from 0.0 to 0.2%. The curves exhibited both linear (V_D < ~0.5 V) and saturation (V_D > 2 V) regions. Compared with the output curves obtained from the IGZO FETs under different gate voltages (V_G's), the piezopotential generated at a strain of 0.2% was comparable to V_G = 0.5 V, representing an I_D of 0.13 μA (Figure 1f). The strain sensitivity of the piezopotential-programmed nonvolatile memory was evaluated by calculating the gauge factor, defined as $(\Delta I_D/I_D)/\varepsilon$. The value for our device was 5202, in far excess of the corresponding values obtained from conventional metal strain gauges (1−5), a state-of-the-art doped-Si strain sensor (~200), and even five times the highest gauge factors reported for carbon nanotube- and ZnO-based piezotronic strain sensors (~1000).[6,35] The ultrahigh gauge factor of our device was attributed to the excellent strain sensitivity of the P(VDF-TrFE) NG and the high on/off current ratio (~10^3) of the IGZO FETs. Note that the minimum detectable and storable strain was found to be 0.005% (Figure S6).

The key requirement for signal memory is the preservation of as-induced charges in the transistor channel by the piezopotential, even after the bending strain has been released. Disconnecting the top electrode of the NG from the ground after applying various strains from 0.06 to 0.2% induced the formation of stable drain current levels (Figure 2a). This persistent current indicated the feasibility of using the piezopotential-powered IGZO FETs as nonvolatile memory devices. The charge carriers in the transistor channel could be preserved by disconnecting the top electrode of the NG from the ground after bending the device (second panel in Figure 2b). Even after releasing the strain, the EDLs formed at both interfaces of the ion gel could not be neutralized because the holes repelled by the enhanced piezopotential could not flow back through the external circuit.[36] The programming process for the nonvolatile memory included three steps: (i) strain application, (ii) ground disconnection, and (iii) data storage, as shown in the left three panels of Figure 2b. Meanwhile, the erasing process could be simply implemented by grounding the top electrode of the NG (reconnecting the top electrode of the NG to the ground), which neutralized the induced charges through the external circuit. Note that a lower power consumption could be achieved because the input potential used for the memorizing/erasing processes was produced from the piezoelectric NGs without any external power source. The programming/erasing time was evaluated to be less than 80 ms (Figure S7). The performances of the piezopotential-programmed nonvolatile memory were further characterized. Figure 2c shows the retention characteristics of the memory devices. The I_D values were measured as a function of the retention time in the program states after the application of five different strains (0.06, 0.09, 0.11, 0.16, and 0.20%). The I_D values were also measured in the erased state. The retention time was determined to exceed 3000 s. A cyclic endurance test was performed, as shown in Figure 2d. The measured I_D values remained invariant over 100 cycles of memorizing/erasing processes.

The device architecture of the piezopotential-programmed nonvolatile memory could be further engineered to explore extended applications. First, the input potentials for programming could be generated by multiple P(VDF-TrFE) NGs coupled to multiple ion gels patterned onto a single IGZO channel. Figure 3a shows a schematic illustration of the resulting device, in which four ion gels were patterned onto the IGZO channel and were connected to each of the extended Al coplanar gate electrode of four P(VDF-TrFE) NGs. The programming characteristics of the devices by the four NGs were investigated. Figure 3b shows the I_D as a function of time, where a 0.2% bending strain was applied to each NG in a step by step manner (from G1 to G1+G2+G3+G4). The stepwise increment in the current level was clearly observed. The output characteristics shown in Figure 3c also indicated that the piezopotentials obtained from the four NGs were effectively coupled to the transistor channel through the four ion gel gate dielectrics; however, the on/off current ratio was only 100 and the current level was limited to be 30 nA, even though a relatively high strain (0.2%) was applied to all four piezoelectric NGs. The poor device performance was explored by measuring the transfer characteristics of the IGZO FETs operated by the gate voltage and the piezopotential, as shown in Figure S8. The on/off current ratios of the devices prepared with four gates were around 100. The poor performances were attributed to the high resistance in the nongated regions of the IGZO channel. The equivalent circuit of the IGZO channel gated by multiple ion gels is illustrated in Figure S9, in which the resistance of the nongated region of the IGZO channel is given by R_0, and the resistances of the ion gel-gated regions are defined as $R_1(V_{G1})$, $R_2(V_{G2})$, $R_3(V_{G3})$, and $R_4(V_{G4})$, respectively. The total resistance between source and drain electrode (R_{total}) was described as $R_{total} = R_0 + R_1(V_{G1}) + R_2(V_{G2}) + R_3(V_{G3}) + R_4(V_{G4})$. The channel conductance of the FET was governed by the nongated regions with extremely high resistances, resulting in a lower on-current level and on/off current ratio.[37]

Second, four piezoelectric NGs were coupled with the FETs through the single ion gel gate dielectric (Figure 3d). The programming characteristics shown in Figure 3e and f indicated that the piezopotentials from four NGs were effectively coupled to the transistor channel through the single ion gel gate dielectrics. The drain current level of 0.34 μA and on/off current ratio of 4.3×10^3 were higher than those obtained from multiple ion gel devices. Although the piezopotentials from the four NGs were coupled to the IGZO FET through a single ion gel gate dielectric, no signal cross-talk was observed because the accumulated ions in the gel could be forced to flow back on demand by selectively grounding each top electrode of the NGs. Figure 3g illustrates the multilevel memorizing/erasing steps applied to the memory devices. The upper panel shows a schematic diagram of the operating process used for multiple memorizing steps. The programming steps, including the strain application, ground disconnection, and data storage, were applied to each NG, respectively. The output signals could be memorized at four different I_D levels as a function of the 0.2% strain applied to each NG. The erasing steps were applied to

DOI: 10.1021/acsnano.6b05895
ACS Nano 2016, 10, 11037−11043

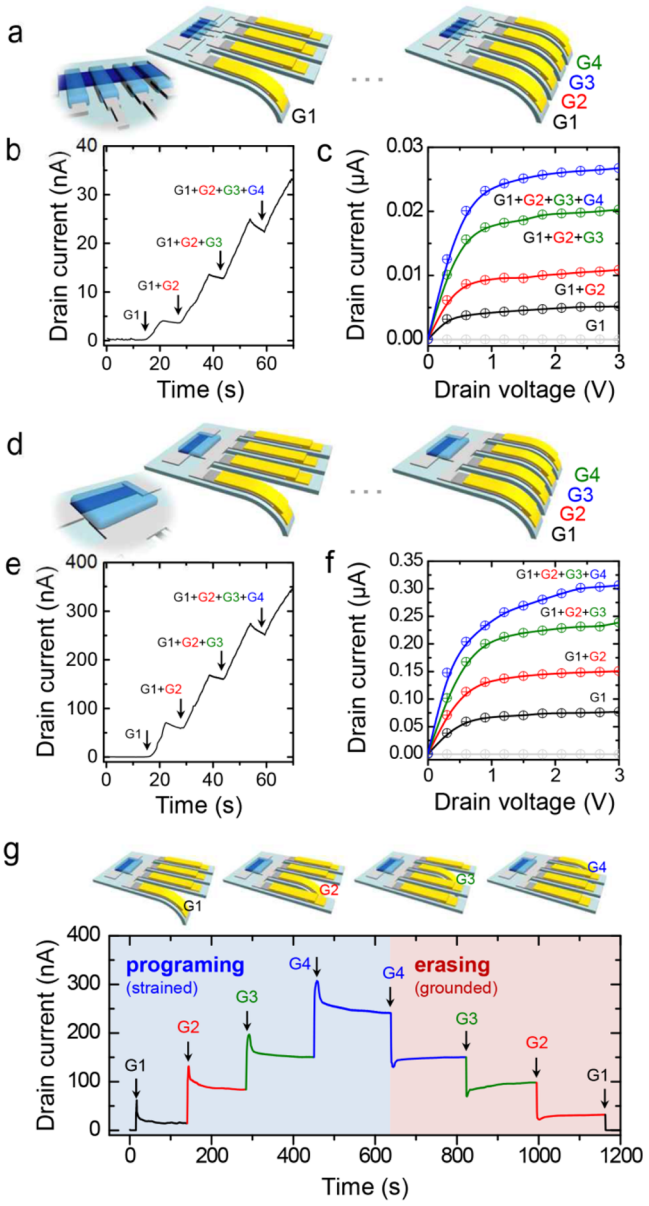

Figure 3. (a) Schematic illustration of the piezopotential-programmed memory prepared with four different ion gels patterned onto a single IGZO channel. (b) Drain current−time plot of the memory (a) programmed by four piezoelectric NGs. (c) Drain current−drain voltage plot of the memory under different NG inputs, from G1 to G1+G2+G3+G4. (d) Schematic illustration of the piezopotential-programmed memory prepared with a single ion gel patterned onto a single IGZO channel. (e) Drain current−time plot of the memory (d) programmed by four piezoelectric NGs. (f) Drain current−drain voltage plot of the memory under different NG inputs, from G1 to G1+G2+G3+G4. (g) Real-time programming and erasing steps applied to the piezopotential-programmed memory.

each NG by reconnecting, one by one, the top electrode of each NG to the ground. The drain current decreased in a stepwise manner as each electrode was grounded, demonstrating that the relevant ions that formed EDLs in the single ion gel could be individually controlled by each NG. The operation mechanism is illustrated in detail using circuit diagrams presented in Figure S10. The multilevel memorizing and erasing properties are of great importance to memory devices that require the storage of multiple mechanical signals from different objects. The devices are potentially useful in biomedical systems involved in monitoring the activities of different organs in human beings.

Finally, the memorizing performances of the piezopotential-programmed nonvolatile memory using objects with a variety of features were investigated. A memory array was prepared using eight FETs and eight NGs aligned next to one another, as shown in Figure 4a. The eight FETs in the memory array exhibited almost identical electrical properties, in which the variations of the maximum current levels were below 0.1 μA (Figure S11). The device array was then fixed on a vertical translation stage, and two types of artificial fingers were attached to a linear translation stage. As the device moved across the object at a speed of 3 mm/s, the piezoelectric NGs were bent at the protruding parts. The height information could be captured and memorized in the device over 3000 s. Three-dimensional (3D) column distributions of the artificial figures are displayed in Figure 4a. The sensing performances of our devices were tested using a target alphabet pattern "OEDL" (representing Organic Electronic Device Lab), as shown in Figure 4b. The output currents measured during moving over the target were monitored over time (Figure 4c). Two-dimensional (2D) color maps of "OEDL" are graphically illustrated, as shown in Figure 4d.

CONCLUSION

In conclusion, a piezopotential-programmed nonvolatile memory was fabricated by integrating a piezoelectric P(VDF-TrFE) NG and an IGZO FET. The memory device was programmed by applying external stains to the NG, followed by subsequent ground disconnection of the top electrode of the NG. By contrast, the stored data could be erased easily by grounding the top electrode of the NG. Multilevel data storage was achieved over 3 orders of magnitude at various external bending strains. The resulting memory devices exhibited good memory performance, including a large programming/erasing current ratio over 10^3, multilevel data storage of 2 bits (over 4 levels), good cyclic stability (over 100 cycles), and good retention stability (over 3000 s). The operation of our piezopotential-programmed nonvolatile memories may not be suitable for high-frequency applications that require fast erasing process in parallel. However, human mechanical motions (with a frequency lower than 10 Hz) can be well harvested to drive our devices. Thus, the memory devices in this paper are potentially useful in low-power, wearable health monitoring systems based on human-robot interactions.

METHODS

Materials Preparation. The IGZO solution was prepared by dissolving indium nitrate hydrate (0.085 M), gallium nitrate hydrate (0.0125 M), and zinc acetate dehydrate (0.0275 M) into 2-methoxyethoxide (10 mL), followed by stirring at 75 °C for 12 h. A ligand exchange reaction occurred between nitrate/acetate and 2-ME, leading to a partial network of metal−oxygen−metal (M−O−M) bonds in the solution. The resulting IGZO film was patterned via the photolithography (AZ 5214) and subsequent wet-etching process (4 vol % LCE-12 in distilled water). The ion gel solution was prepared by mixing poly(ethylene glycol) diacrylate (PEGDA), 2-hydroxy-2-methylpropiophenone (HOMPP), and 1-ethyl-3-methylimidazolium bis(trifluoromethanesulfonyl)imide ([EMIM][TFSI]) (the weight ratio was 7:3:90). HOMPP worked as a photoinitiator to generate radicals that reacted with the acrylates in the PEGDA monomers to initiate polymerization under UV exposure. The P(VDF-TrFE)

DOI: 10.1021/acsnano.6b05895
ACS Nano 2016, 10, 11037−11043

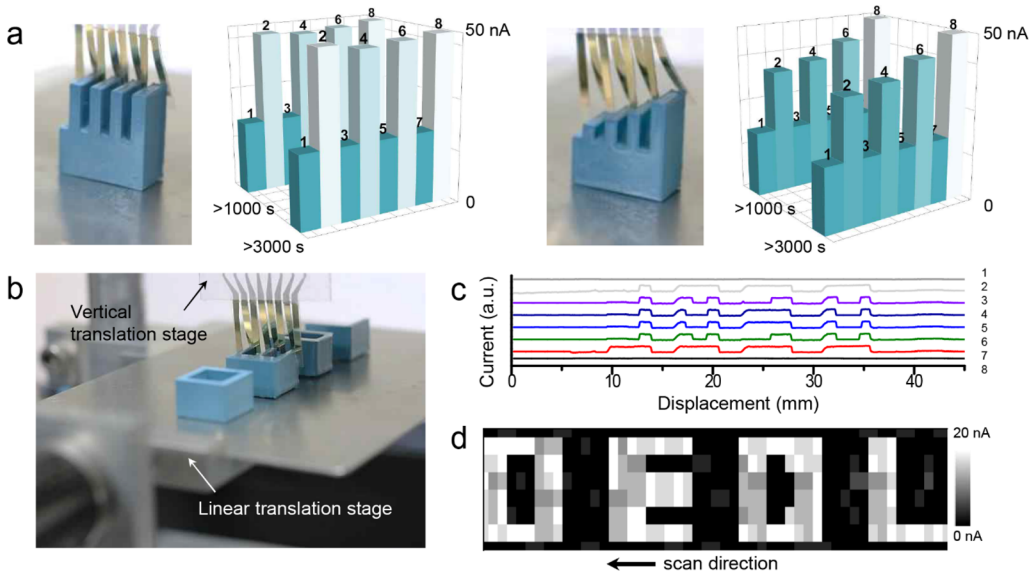

Figure 4. (a) Programming characteristics of the piezopotential-programmed memory array by two types of artificial fingers. (b) Sensing performances of the piezopotential-programmed memory array using the target alphabet pattern "OEDL".

copolymer (ARKEMA Inc.) was dissolved in N, N-dimethylformamide (DMF) at a ratio of 20 wt % and then stirred overnight.

Device Fabrication. The polyethylene terephthalate (PET) substrate was cleaned with acetone, isopropyl alcohol, and DI water. A 50 nm thick Al electrode was deposited using a thermal evaporation system. After treating with UV-ozone over 30 min, the IGZO solution was spin-coated onto the substrate, followed by application of deep UV photoannealing (UV253H, Filgen) under N_2 purging. The light source was a low-pressure mercury lamp with two main emission peaks at 253.7 nm (90%) and 184.9 nm (10%). The sintered IGZO film was then patterned using photolithography and acid etching. The P(VDF-TrFE) layer was patterned through a conformable polyurethane arylate (PUA) mask. Au electrodes (50 nm) were then evaporated thermally on top of the P(VDF-TrFE). The electrical poling process for the P(VDF-TrFE) film was carried out by applying an electric field (100 $MV \cdot m^{-1}$) between the top Au and bottom Al electrodes for 30 min. Finally, the ion gel gate dielectrics were photopatterned across the IGZO channel and a portion of Al coplanar gate electrode.

Measurements. The electrical properties of the memories were characterized using a source-meter (Keithley 2400). External strains were applied using a home-built bending system with a step motor controller. The output voltages and currents of the piezoelectric NGs were measured using an oscilloscope (DSO 1204A, Agilent) and a low-noise current preamplifier (SR570, Stanford Research Systems, Inc.).

ASSOCIATED CONTENT

Supporting Information

The Supporting Information is available free of charge on the ACS Publications website at DOI: 10.1021/acsnano.6b05895.

SEM image of P(VDF-TrFE) film; output performance of P(VDF-TrFE) piezoelectric NG; transfer characteristics of ion gel-gated IGZO FETs; calculation of strain applied in length direction (ε_y); operating mechanism of piezopotential-powered IGZO FETs with ion gel gate dielectrics; minimum detectable strain (0.005%) of piezopotential-programmed memory; I_D-V_G plots of four ion gel-gated IGZO FETs; I_D−time plots of four ion gel-gated IGZO FET under applied bending strain at a speed of 0.5 mm/s; schematic illustration of IGZO FETs gated by four ion gel and equivalent circuit diagram of the IGZO channel; detail operation mechanism of piezopotential-programmed memory; transfer characteristics of eight IGZO FETs in memory array (PDF)

AUTHOR INFORMATION

Corresponding Author

*E-mail: jhcho94@skku.edu.

ORCID

Zhong Lin Wang: 0000-0002-5530-0380

Jeong Ho Cho: 0000-0002-1030-9920

Notes

The authors declare no competing financial interest.

ACKNOWLEDGMENTS

J.H.C. and D.H.K. were supported financially by a grant from the Center for Advanced Soft Electronics (CASE) under the Global Frontier Research Program (2013M3A6A5073177 and 2014M3A6A5060932), Korea. Q.S. was supported financially by the "thousands talents" program for pioneer researcher and his innovation team, National Natural Science Foundation of China (Grand No. 51605034) and national key R&D project from Minister of Science and Technology (2016YFA0202703), China.

REFERENCES

(1) Wang, Z. L. Progress in Piezotronics and Piezo-Phototronics. *Adv. Mater.* **2012**, *24*, 4632−4646.

(2) Wang, Z. L. Piezopotential Gated Nanowire Devices: Piezotronics and Piezo-Phototronics. *Nano Today* **2010**, *5*, 540−552.

(3) Xu, S.; Qin, Y.; Xu, C.; Wei, Y.; Yang, R.; Wang, Z. L. Self-Powered Nanowire Devices. *Nat. Nanotechnol.* **2010**, *5*, 366−373.

(4) Wang, X. Piezoelectric Nanogenerators-Harvesting Ambient Mechanical Energy at the Nanometer Scale. *Nano Energy* **2012**, *1*, 13−24.

(5) Sun, Q.; Seung, W.; Kim, B. J.; Seo, S.; Kim, S. W.; Cho, J. H. Active Matrix Electronic Skin Strain Sensor Based on Piezopotential-Powered Graphene Transistors. *Adv. Mater.* **2015**, *27*, 3411−3417.

(6) Zhou, J.; Gu, Y.; Fei, P.; Mai, W.; Gao, Y.; Yang, R.; Bao, G.; Wang, Z. L. Flexible Piezotronic Strain Sensor. *Nano Lett.* **2008**, *8*, 3035−3040.

DOI: 10.1021/acsnano.6b05895
ACS Nano 2016, 10, 11037−11043

(7) Pan, C.; Yu, R.; Niu, S.; Zhu, G.; Wang, Z. L. Piezotronic Effect on the Sensitivity and Signal Level of Schottky Contacted Proactive Micro/Nanowire Nanosensors. *ACS Nano* **2013**, *7*, 1803−1810.
(8) Yu, R.; Pan, C.; Wang, Z. L. High Performance of ZnO Nanowire Protein Sensors Enhanced by the Piezotronic Effect. *Energy Environ. Sci.* **2013**, *6*, 494−499.
(9) Lee, M.; Bae, J.; Lee, J.; Lee, C.-S.; Hong, S.; Wang, Z. L. Self-Powered Environmental Sensor System Driven by Nanogenerators. *Energy Environ. Sci.* **2011**, *4*, 3359−3363.
(10) Yeh, P. H.; Li, Z.; Wang, Z. L. Schottky-Gated Probe-Free ZnO Nanowire Biosensor. *Adv. Mater.* **2009**, *21*, 4975−4978.
(11) Wei, T.-Y.; Yeh, P.-H.; Lu, S.-Y.; Wang, Z. L. Gigantic Enhancement in Sensitivity Using Schottky Contacted Nanowire Nanosensor. *J. Am. Chem. Soc.* **2009**, *131*, 17690−17695.
(12) Chen, X.; Xu, S.; Yao, N.; Shi, Y. 1.6 V Nanogenerator for Mechanical Energy Harvesting Using PZT Nanofibers. *Nano Lett.* **2010**, *10*, 2133−2137.
(13) Yang, R.; Qin, Y.; Li, C.; Zhu, G.; Wang, Z. L. Converting Biomechanical Energy into Electricity by a Muscle-Movement-Driven Nanogenerator. *Nano Lett.* **2009**, *9*, 1201−1205.
(14) Pan, C.; Dong, L.; Zhu, G.; Niu, S.; Yu, R.; Yang, Q.; Liu, Y.; Wang, Z. L. High-Resolution Electroluminescent Imaging of Pressure Distribution Using a Piezoelectric Nnanowire LED Array. *Nat. Photonics* **2013**, *7*, 752−758.
(15) Wang, X.; Zhang, H.; Yu, R.; Dong, L.; Peng, D.; Zhang, A.; Zhang, Y.; Liu, H.; Pan, C.; Wang, Z. L. Dynamic Pressure Mapping of Personalized Handwriting by a Flexible Sensor Matrix Based on the Mechanoluminescence Process. *Adv. Mater.* **2015**, *27*, 2324−2331.
(16) Wu, W.; Wen, X.; Wang, Z. L. Taxel-Addressable Matrix of Vertical-Nanowire Piezotronic Transistors for Active and Adaptive Tactile Imaging. *Science* **2013**, *340*, 952−957.
(17) Wang, Z. L.; Wu, W. Nanotechnology-Enabled Energy Harvesting for Self-Powered Micro-/Nanosystems. *Angew. Chem., Int. Ed.* **2012**, *51*, 11700−11721.
(18) Ho, D. H.; Sun, Q.; Kim, S. Y.; Han, J. T.; Kim, D. H.; Cho, J. H. Stretchable and Multimodal All Graphene Electronic Skin. *Adv. Mater.* **2016**, *28*, 2601−2608.
(19) Kim, S. Y.; Park, S.; Park, H. W.; Park, D. H.; Jeong, Y.; Kim, D. H. Highly Sensitive and Multimodal All-Carbon Skin Sensors Capable of Simultaneously Detecting Tactile and Biological Stimuli. *Adv. Mater.* **2015**, *27*, 4178−4185.
(20) Kim, D.-H.; Lu, N.; Ma, R.; Kim, Y.-S.; Kim, R.-H.; Wang, S.; Wu, J.; Won, S. M.; Tao, H.; Islam, A.; et al. Epidermal Electronics. *Science* **2011**, *333*, 838−843.
(21) Kim, J.; Lee, M.; Shim, H. J.; Ghaffari, R.; Cho, H. R.; Son, D.; Jung, Y. H.; Soh, M.; Choi, C.; Jung, S.; et al. Stretchable Silicon Nanoribbon Electronics for Skin Prosthesis. *Nat. Commun.* **2014**, *5*, 5747−5747.
(22) Lipomi, D. J.; Vosgueritchian, M.; Tee, B. C.; Hellstrom, S. L.; Lee, J. A.; Fox, C. H.; Bao, Z. Skin-Like Pressure and Strain Sensors Based on Transparent Elastic Films of Carbon Nanotubes. *Nat. Nanotechnol.* **2011**, *6*, 788−792.
(23) Wang, C.; Hwang, D.; Yu, Z.; Takei, K.; Park, J.; Chen, T.; Ma, B.; Javey, A. User-Interactive Electronic Skin for Instantaneous Pressure Visualization. *Nat. Mater.* **2013**, *12*, 899−904.
(24) Kaltenbrunner, M.; Sekitani, T.; Reeder, J.; Yokota, T.; Kuribara, K.; Tokuhara, T.; Drack, M.; Schwödiauer, R.; Graz, I.; Bauer-Gogonea, S.; et al. An Ultra-Lightweight Design for Imperceptible Plastic Electronics. *Nature* **2013**, *499*, 458−463.
(25) Son, D.; Lee, J.; Qiao, S.; Ghaffari, R.; Kim, J.; Lee, J. E.; Song, C.; Kim, S. J.; Lee, D. J.; Jun, S. W.; et al. Multifunctional Wearable Devices for Diagnosis and Therapy of Movement Disorders. *Nat. Nanotechnol.* **2014**, *9*, 397−404.
(26) Sekitani, T.; Yokota, T.; Zschieschang, U.; Klauk, H.; Bauer, S.; Takeuchi, K.; Takamiya, M.; Sakurai, T.; Someya, T. Organic Nonvolatile Memory Transistors for Flexible Sensor Arrays. *Science* **2009**, *326*, 1516−1519.
(27) Kim, S.-J.; Lee, J.-S. Flexible Organic Transistor Memory Devices. *Nano Lett.* **2010**, *10*, 2884−2890.
(28) Son, D.; Koo, J. H.; Song, J.-K.; Kim, J.; Lee, M.; Shim, H. J.; Park, M.; Lee, M.; Kim, J. H.; Kim, D.-H. Stretchable Carbon Nanotube Charge-Trap Floating-Gate Memory and Logic Devices for Wearable Electronics. *ACS Nano* **2015**, *9*, 5585−5593.
(29) Jang, S.; Hwang, E.; Lee, J. H.; Park, H. S.; Cho, J. H. Graphene-Graphene Oxide Floating Gate Transistor Memory. *Small* **2015**, *11*, 311−318.
(30) Wu, W.; Wang, Z. L. Piezotronic Nanowire-Based Resistive Switches as Programmable Electromechanical Memories. *Nano Lett.* **2011**, *11*, 2779−2785.
(31) Zhang, C.; Li, J.; Han, C. B.; Zhang, L. M.; Chen, X. Y.; Wang, L. D.; Dong, G. F.; Wang, Z. L. Organic Tribotronic Transistor for Contact-Electrification-Gated Light-Emitting Diode. *Adv. Funct. Mater.* **2015**, *25*, 5625−5632.
(32) Kim, Y.-H.; Heo, J.-S.; Kim, T.-H.; Park, S.; Yoon, M.-H.; Kim, J.; Oh, M. S.; Yi, G.-R.; Noh, Y.-Y.; Park, S. K. Flexible Metal-Oxide Devices Made by Room-Temperature Photochemical Activation of Sol-Gel Films. *Nature* **2012**, *489*, 128−132.
(33) Kim, J. H.; Hong, S. H.; Seong, K. d.; Seo, S. Fabrication of Organic Thin-Film Transistors on Three-Dimensional Substrates Using Free-Standing Polymeric Masks Based on Soft Lithography. *Adv. Funct. Mater.* **2014**, *24*, 2404−2408.
(34) Hwang, S. K.; Bae, I.; Kim, R. H.; Park, C. Flexible Non-Volatile Ferroelectric Polymer Memory with Gate-Controlled Multilevel Operation. *Adv. Mater.* **2012**, *24*, 5910−5914.
(35) Cao, J.; Wang, Q.; Dai, H. Electromechanical Properties of Metallic, Quasimetallic, and Semiconducting Carbon Nanotubes Under Stretching. *Phys. Rev. Lett.* **2003**, *90*, 157601.
(36) Lee, J.-H.; Lee, K. Y.; Kumar, B.; Tien, N. T.; Lee, N.-E.; Kim, S.-W. Highly Sensitive Stretchable Transparent Piezoelectric Nanogenerators. *Energy Environ. Sci.* **2013**, *6*, 169−175.
(37) Burke, A.; Carrad, D.; Gluschke, J.; Storm, K.; Fahlvik Svensson, S.; Linke, H.; Samuelson, L.; Micolich, A. InAs Nanowire Transistors with Multiple, Independent Wrap-Gate Segments. *Nano Lett.* **2015**, *15*, 2836−2843.

DOI: 10.1021/acsnano.6b05895
ACS Nano 2016, 10, 11037−11043